Periodica Polytechnica Civil Engineering, 69(3), pp. 944–953, 2025

Estimation of the Constitutive Relationship between Impact Resistance and Compressive Strength in Sandstones

Benedek A. Lógó[1*], Balázs Vásárhelyi[1]

[1] Department of Engineering Geology and Geotechnics, Faculty of Civil Engineering, Budapest University of Technology and Economics, Műegyetem rkp. 3., H-1111 Budapest, Hungary
[*] Corresponding author, e-mail: logo.benedek@emk.bme.hu

Received: 21 February 2025, Accepted: 16 June 2025, Published online: 07 July 2025

Abstract

A series of experiments were performed to investigate the relation between the impact resistance and the compressive strength of sedimentary rocks. The experiments were conducted by the use of Charpy hammer. As a result of these series of experiments an analytical relation was elaborated between the impact resistance and the compressive strength of sedimentary rocks. An envelope domain is presented as an upper and lower bound for this relation, respectively. In the case of the samples, regardless of temperature and saturation states, the impact work values fell within the range bounded by these limit lines (two straight lines). This makes it possible to obtain an estimated strength value by the help of the tests performed in this way only by determining the density and impact work. Measurements performed at different temperatures and saturation states showed that the temperature of the sample at temperatures between −12 °C and 20 °C only minimally affects the result. The water saturation of the sample has a much greater effect on the impact resistance.

Keywords

sedimentary rock, impact work, Charpy impact test, compressive strength, impact resistance

1 Introduction

Charpy already recognized that the collision energy of solid bodies and the yield strength of metals are related [1]. The Charpy pendulum is used to measure the impact energy, as this test is a well-developed and long-used procedure for other materials, especially for metals. For example, recently a lot of researches have been done to determine the impact resistance of various metals [2], polymers [3] and glass composites [4], but only a few on natural stones. Most of the available researches also refer to igneous rocks, mostly various granites [5] were examined. The strength of the method is that it does not require any complicated equipment, it can be performed easily, so it can be used widely with natural building materials, as well.

Based on the international literature, many researches have already been carried out to determine the value of the compressive strength by the help of different simple test methods. Among them Cargill and Shakoor [6] evaluated measurement methods suitable for estimating the compressive strength of stones. In this case, he used point strength measurement, Schmidt hammer strength estimation and Los Angeles wear test to determine the compressive strength. Zorlu et al. [7] looked for a solution in the case of sandstones on how to develop a method that can easily give the compressive strength. This is necessary aspect for practice, since even though compressive strength is one of the most important mechanical parameters, it is very difficult to create a test specimen of the right size and condition. This is especially true advice if the examined rock is fractured. Çobanoğlu and Çelik [8] investigated the relationships between uniaxial compressive strength and point strength test, P-wave velocity and the rebound number of Schmidt hammer strength estimation, as well as the effects of core gauge size. Fener et al. [9] compared the various tests suitable for estimating the uniaxial compressive strength.

Borg [10] used the Charpy impact test in his research for rock drilling and modeling the dynamic effects that occur there, Furuzumi et al. [11, 12] investigated the dynamic fracture toughness of rocks and the change in crack propagation speed. Komurlu [5] examined 13 different granite samples in a way that could also monitor the formation of the fracture pattern, Durif et al. [13] developed a real-time method capable of following the formation and propagation

Cite this article as: Lógó, B. A., Vásárhelyi, B. "Estimation of the Constitutive Relationship between Impact Resistance and Compressive Strength in Sandstones", Periodica Polytechnica Civil Engineering, 69(3), pp. 944–953, 2025. https://doi.org/10.3311/PPci.40270

of cracks using the impact test. He et al. [14] investigated the relationship between the change in loading speed and the value of compressive strength, Kharchenko et al. [15] investigated impact resistance as a result of changes in temperature and impact speed. Zhang and Zhao [16] aim to discuss the development and state of the art of dynamic testing techniques and dynamic mechanical behavior of rock materials. Zou and Wong [17], although not with a Charpy impact test, tested marble for dynamic loading.

Impact strength testing for stones was invented by Protodyakonov [18] in 1962, and then Evans and Pomeroy [19] developed the measuring device for it. Unlike the Charpy pendulum [1, 20, 21], this does not test a single specimen, but a specific weight is dropped 20 times from a height determined for a 100 g sample. It specifies the amount of impact energy based on the stones remaining within the size range. In his study of the method, Kahraman [22] explained that there is no relationship between the resulting impact energy and the one-way compressive strength.

The purpose of the series of this experiment is to find a relationship that shows the relationship between the impact resistance of rocks and the compressive strength. In the present research, we looked at the impact resistance of only one sedimentary rock, the green sandstone. The tests were compiled in such a way that the condition of the test specimens covered the conditions occurring in nature as best as possible. For this reason, the tests were carried out both in air-dry and saturated conditions with different temperatures. In Section 2 the used equipment and the theoretical background are introduced briefly. The flow of the tests is presented in Section 3. The general finding and the elaborated mathematical formulations are given in this section, too. The main finding of this work can be found in Section 4.

2 The Charpy test equipment and its theoretical background

Impact energy can be used as a measure of mechanical behavior of solid bodies, as indicated above. One of the most commonly used equipment to determine this energy is the Charpy hammer in case of metals. Since the Charpy-test is not a common experience in rock mechanics, it is important to know its theoretical background. One can find review information in Lógó and Vásárhelyi's [23] paper. When the test specimen is broken, some of the pendulum's kinetic energy is consumed, and the remainder continues to swing the pendulum. The impact work is the impact energy used to break the test piece, which can be read on the scale of the equipment.

As shown in Fig. 1, the pendulum of mass m attached to the end of the rod of length R starts from the position of height h_0. In this case, the potential energy of the position is:

$$E_0 = m \times g \times h_0 \,. \tag{1}$$

After the impact, the pendulum (Fig. 2) swings to a position of height h_1, where the potential energy of the position is:

$$E_1 = m \times g \times h_1 \,. \tag{2}$$

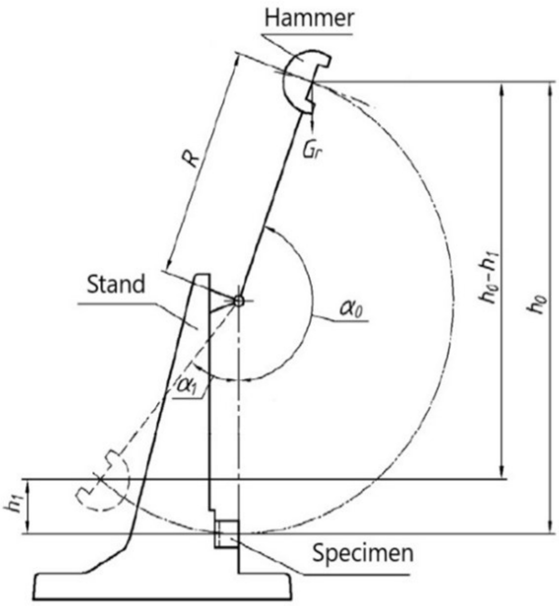

Fig. 1 The theoretical figure of the pendulum

Fig. 2 The Charpy pendulum

The difference between the positional potential energies gives the value of the energy used to break the test piece, i.e. the value of the collision work (W).

$$W = E_0 - E_1 = m \times g \times (h_0 - h_1) \quad (3)$$

The exact measurement of the height during the test can often be solved with difficulty, therefore the value of the heights can be determined with the help of the initial (α_0) and (α_1) overshoot angles.

$$W = m \times g \times R \times (\cos\alpha_0 - \cos\alpha_1) \quad (4)$$

Impact bending machines are already designed in such a way that the value of the impact work and the magnitude of the overshoot angle can be read directly by the help of an indicator, so the value of the impact work can be easily calculated by substituting it into Eq. (4).

During the measurements, it is strived to obtain as many measurement results as possible from a single test specimen, so at first the mechanical properties of each sample determined using non-destructive testing methods. Initially the test specimens are examined by a device (ultrasound) suitable for measuring P and S waves, and then, from the results obtained, the P-wave modulus (Eq. (5)), shear modulus (Eq. (6)), Poisson's ratio (Eq. (7)) and deformation modulus (Eq. (8)) are determined by using the following relationships:

$$M_{din} = \rho \times V_p^2 \quad (5)$$

$$G_{din} = \rho \times V_s^2 \quad (6)$$

$$v_{din} = \frac{V_p^2 - 2 \times V_s^2}{2 \times (V_p^2 - V_s^2)} \quad (7)$$

$$E_{din} = 2G(1 + v) \quad (8)$$

where:

- M: P-wave modulus,
- ρ: the density of the specimen,
- V_p: P-wave velocity
- G: shear modulus,
- v: Poisson's ratio,
- V_s: S-wave velocity,
- E: stands for dynamic Young's modulus.

In the following we used the theory introduced above.

2.1 Temperature dependence

As it was indicated that the Charpy impact test was developed primarily for the qualification of metals, where the temperature of the sample to be tested greatly influences on the degree of impact resistance. As it can be seen in Fig. 3, the most intense change in impact work of this type of metal occurs in the range −50 °C–50 °C. Since traditional engineering tasks are also within this range, we will also examine the test specimens in this temperature range. The examined samples were therefore measured with the Charpy impact test at temperatures between −12 °C and 20 °C.

3 Material description and test preparations

During the experiments, green sandstones were examined in various states. The green sandstone, also known as glauconite sandstone, is a type of sandstone that often contains large amounts of glauconite (potassium-iron clay mineral) aggregates. It forms in the shallow sea, i.e. at a maximum depth of 400 m, usually in relatively warm water (15–20 °C). The geometries of more than a hundred specimens were designed so that the size of the grains that make up the sandstone affects the place of the fracture and the direction of the fracture as little as possible. The test pieces (Figs. 4 and 5) are 25 × 25 × 60 mm in size, the geometric deviations are less than 1 mm for any size. The standard deviation of the sizes of the individual sides is shown in the following picture: 0.4 mm and 0.5 mm for the two shorter sides, while 0.6 mm for the 60 mm long side. It is commonly known that the measure of saturation

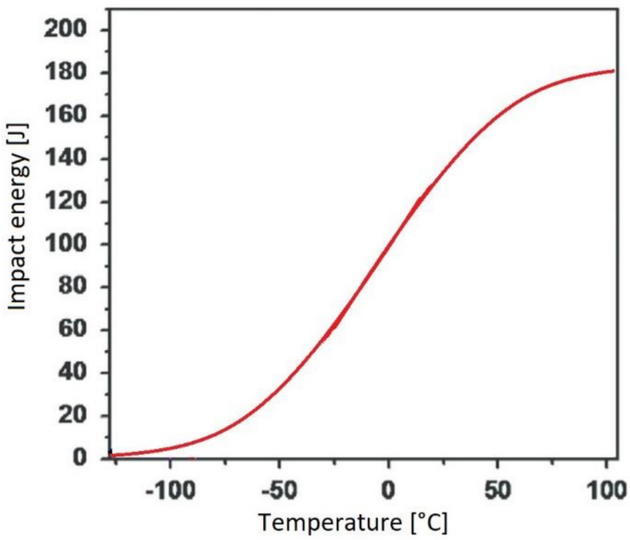

Fig. 3 Effect of temperature change on steel [24]

Fig. 4 Green sandstone specimen

Fig. 5 Specimen after the test

has an effect on the mechanical behavior of rocks. During the measurement, the specimens were either saturated with water or air-dried, and we also examined the temperature as an influencing factor. As it was indicated the examined samples were measured at the temperatures between −12 °C and 20 °C. The number of the specimens are cc. 25 in each group.

The specimens were investigated first by non-destructive tests and then destructive tests. During the non-destructive tests specific mechanical properties of specimens (Table 1) i.e., density, P and S wave velocity of the ultrasound wave, temperature, water absorption, geometrical dimensions were determined. The destructive tests include the impact test and the uniaxial compressive test. In this case as well, as much data as possible were determined from one sample.

In order to do this, we first performed the Charpy pendulum test, and then the uniaxial compressive strength test (Fig. 6). The results obtained in this way were analyzed using statistical methods.

4 Results of the tests and derived formulations

The obtained measurement results were compared with each other according to several different aspects. Our goal is to be able to find a correlation between the impact energy and some property or properties of the sample as widely as possible. Additionally, the secondary goal is to find physical quantities which are fundamental ones for daily practice in using rocks. When selecting these physical quantities, we tried to give priority to data that can be easily determined, so that neither special instruments nor complicated procedures are needed for the applicability of the obtained correlation.

Table 1 Properties of the specimens – statistic calculations

Physical quantity		dry frozen	dry normal	saturated frozen	saturated normal
M (GPa)	average	17.80	17.78	17.75	17.73
	standard deviation	1.34	1.14	1.14	0.02
ν (-)	average	0.25	0.25	0.25	0.25
	standard deviation	0.02	0.02	0.02	0.02
E (GPa)	average	13.78	13.30	13.73	13.56
	standard deviation	0.82	0.68	0.70	0.73
G (GPa)	average	5.52	5.33	5.49	5.44
	standard deviation	0.27	0.25	0.24	0.26

Fig. 6 Uniaxial compressive strength test

The examined sandstone (Figs. 4–6) is fine-grained and can be considered homogeneous from the point of view of the measurement, as evidenced by the fact that the highest deviation in the density measurement is only 0.03 g/dm^3 (Table 2). In the case of impact work, the standard deviation is already larger, this is partly due to the material of the green sandstone. Since this is a sedimentary stone, the settlement direction of the individual layers could be detected during the measurements, despite the fact that it was not noticeable to any extent with the naked eye. In the case of samples at normal temperature, there is approximately a 35% difference between the impact work of saturated and air-dried samples. In this case, the higher values were obtained

Table 2 Average density and impact work values of the samples in different conditions

		dry frozen	dry normal	saturated frozen	saturated normal
Density (g/cm^3)	average	2.42	2.41	2.41	2.41
	standard deviation	0.03	0.03	0.03	0.02
Impact work (J)	average	8.63	10.22	10.71	7.55
	standard deviation	2.71	1.84	0.63	2.07

during the measurement of air-dried specimens. In the case of frozen samples, this difference was around 24%. Here, on the other hand, the higher impact work values were obtained during the examination of the saturated samples.

It is known in rock mechanics, that the saturated samples are weaker in general. This trend is even more valid in case of sedimentary stones. Our experiments prove with specific numbers for green sandstone this phenomenon. The reliability of the impact resistance test is on the same level as the Schmidt hammer test or the Poldi hammer test in mechanics. The impact resistance of frozen, saturated specimens are strongly affected by the impact resistance of ice. It could lead, that the original 35% being turned to 24%. On the other side it could have practical meaning, because the ground freezing methods are quite common in the excavations.

During the evaluation of the measurement results, we obtained the result that, in the case of the examined samples, the value determined by the quotient of impact energy, density and compressive strength has a mathematically well-describable relationship with each other.

In case of the samples, regardless of temperature and saturation state, the impact work values fell within the range bounded by two straight lines (Fig. 7 (a), (b)) which can used as envelope lines of impact "resistance" of the samples. This makes it possible to obtain an estimated strength value with the help of the tests performed in this way only by determining the density and impact work. Before defining each limit, we used statistical methods to check whether each value was greater than the average minus three times the standard deviation, or if it was smaller than the sum of the average and three times the standard deviation. If a sample does not fit into this range, it cannot be taken into account when establishing the limits. In the case of the examined green sandstone, all measured values were in the appropriate range, so when setting up the boundary curves, it was only necessary to find the straight line that starts from the origin and passes through the two outermost elements of the set of points.

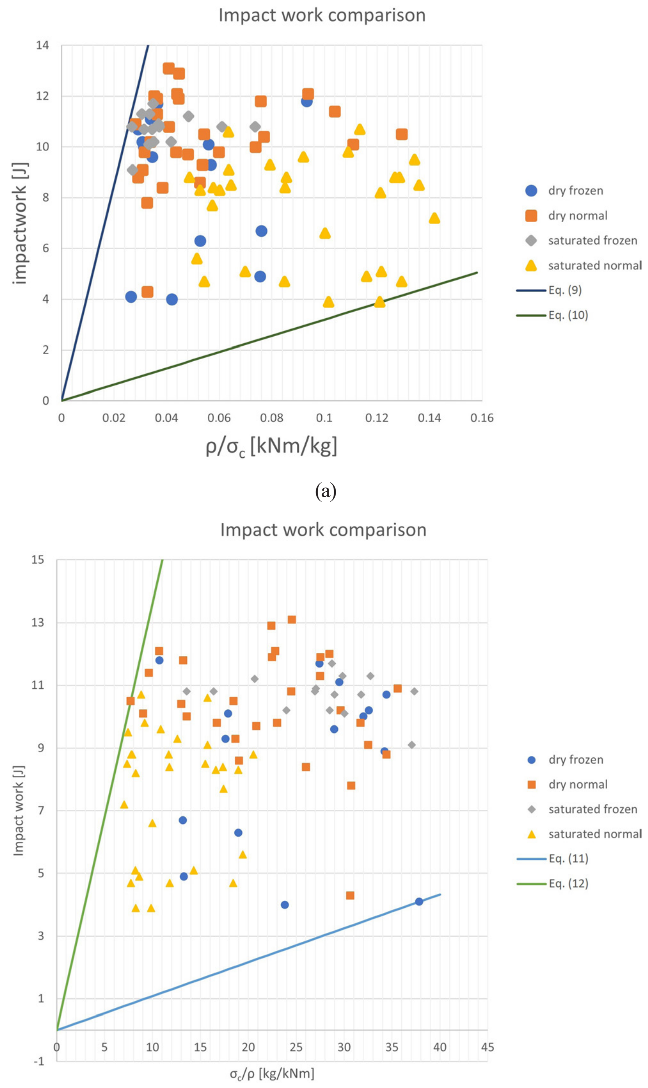

(b)

Fig. 7 Impact work comparison, envelope lines: (a) ρ/σ_c, (b) σ_c/ρ

Based on this, if the density divided by σ_c (Fig. 7 (a)), the upper limit of the values is described by Eq. (9), while the lower limit is given by Eq. (10).

$$\sigma_c = 425 \times \rho / W \tag{9}$$

$$\sigma_c = 32 \times \rho / W \tag{10}$$

Here W means impact work, ρ is the density of the specimen, σ_c is the compressive strength of the specimen means.

If the impact work is compared with the quotient of σ_c and density (Fig. 7 (b)), then the limits in Eq. (11) and Eq. (12) are given.

$$\sigma_c = 9.23 \times \rho \times W \tag{11}$$

$$\sigma_c = 0.736 \times \rho \times W \tag{12}$$

If we examine samples with the same temperature but different saturation states (Fig. 8), it can be seen that the measured values are divided into two clearly distinguishable ranges according to the water saturation state of the sample A function can be fitted to the boundary. One can use any mathematical methods to determine this curve. We select the Langrage-approximations to calculate it. The solution of the problem above can be obtained by the use of n^{th} degree of Langrange interpolation polynomials,

$$P_n(x_i) = \sum_{i=1}^{n+1} y_i L_i(x); \tag{13}$$

where the i^{th} Lagrange polynomial is

$$L_i(x) = \frac{(x-x_1)(x-x_2)\ldots(x-x_{i-1})(x-x_{i+1})\ldots(x-x_{n+1})}{(x_i-x_1)\ldots(x_i-x_{i-1})(x_i-x_{i+1})\ldots(x_i-x_{n+1})}$$
$$L_i(x) = \begin{cases} 0; & \text{if } x = x_j;\; j = 1,2,\ldots,i-1,i+1,\ldots,n+1 \\ 1; & \text{if } x = x_i \end{cases} \tag{14}$$

here n+1 means the number of the available points (here the experimentally determined values).

Introducing $\omega(x) = (x - x_1)(x - x_2) \ldots (x - x_{n+1})$ the base polynomial can be calculated by

$$L_i(x) = \frac{\omega(x)}{(x-x_i)\,\omega'(x_i)}. \tag{15}$$

Since we want to separate two ranges from each other, we can only use a curve with an even degree during the procedure, since in the case of functions with an odd degree, the nature of the curve is not suitable for dividing the measurement results into ranges in our case. As a result, in each case at least three points had to be selected to determine the curve. A point on the curve is the point where the product of the impact work and the quotient of σ_c and ρ is the maximum. The other point is where the quotient of the impact work and the quotient of σ_c and ρ is the minimum. The intermediate point is the value closest to the average the quotient of σ_c and ρ of the two points.

Neglecting the details of the calculation the Lagrange approximation, in the case of samples with a normal temperature, i.e. 22 °C the boundary function between the two states is described by Eq. (16):

$$W = -0.00889 \times \left(\frac{\rho}{\sigma_c}\right)^2 + 0.070724 \times \frac{\rho}{\sigma_c} + 10.48447\,. \tag{16}$$

The relation given by Eq. (16) delimiting the two states was determined from the data using a Lagrange approximation can be seen in Fig. 8 in case of non-frozen dry and saturated samples.

In addition, a comparison is performed to find the relative error in these approximations (linear and polynomial) of the compressive (tensile) strength. This would greatly facilitate the development of an on-site inspection that is easy and quick to perform to get the unknown strength value if the specific impact work values (min. 3) are known.

This comparison was also performed for samples with the same saturation state but different temperatures. The test specimens have a temperature between −12 °C and 20 °C and are saturated with water. The comparison (Fig. 9) showed a similar trend as in the previous case, it can also be observed that the measurement results are divided into two groups. Here, the boundary function is described by Eq. (17) obtained in a similar way:

$$W = -0.03083 \times \left(\frac{\rho}{\sigma_c}\right)^2 + 0.742696 \times \frac{\rho}{\sigma_c} + 6.548063\,. \tag{17}$$

One can see the evaluation of the impact work in function of normalized compressive strength in Fig. 9.

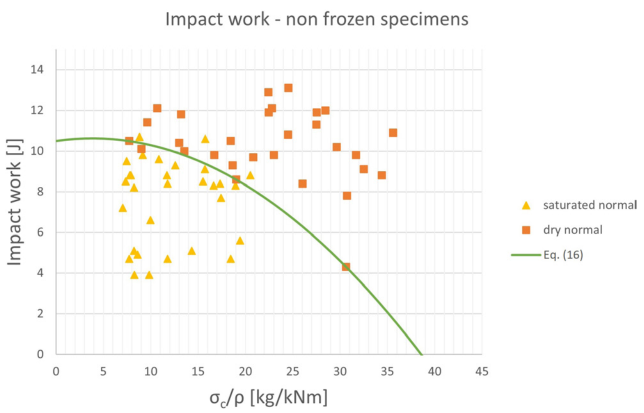

Fig. 8 Non frozen (normal) specimen's impact work in function of normalized compressive strength

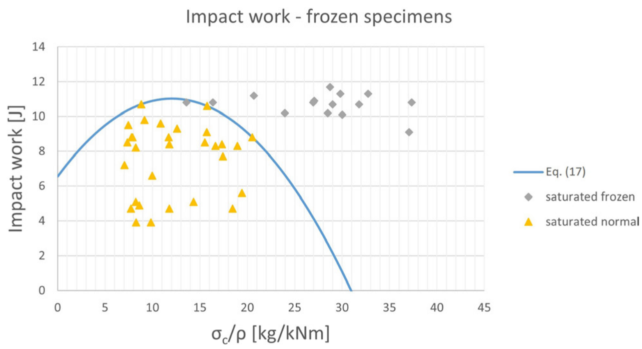

Fig. 9 Frozen specimen's impact work in function of normalized compressive strength

The boundaries (envelope lines) of the different states (Figs. 10, 11) can also be easily defined. These are given by Eq. (9) and Eq. (18) in case air-dry, not frozen specimens, Eq. (9) and Eq. (19) in case of air-dry frozen samples, Eq. (10) and Eq. (20) in case saturated, not frozen specimens, and in case of saturated frozen samples Eq. (9) and Eq. (21).

$$\sigma_c = 78 \times \rho \times W \tag{18}$$

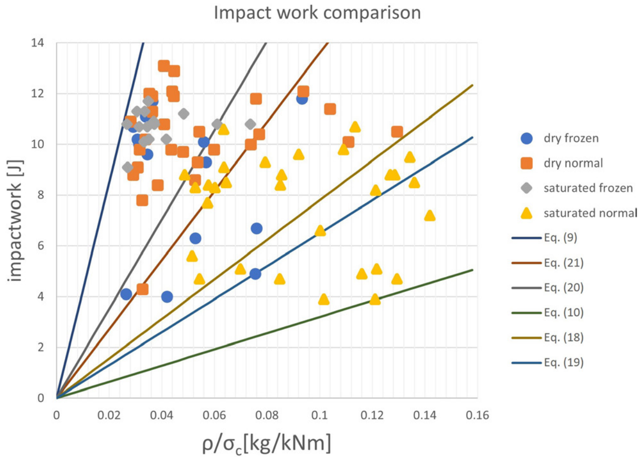

Fig. 10 The boundaries (envelope lines) of the different states of specimens

$$\sigma_c = 65 \times \rho \times W \tag{19}$$

$$\sigma_c = 176 \times \rho \times W \tag{20}$$

$$\sigma_c = 136 \times \rho \times W \tag{21}$$

In this temperature range, based on the test results, there was no difference between the individual results to the extent expected for metals. Based on the results shown in Table 3, it can be seen that the difference is 0.3 J for the smallest values, and 1.3 J for the maximum impact values in the air-dry case. If the samples are saturated with water, it can be seen that significantly different values are obtained during the test when they are frozen, however almost no different between the medians and the average of the impact works in case of dry normal and saturated frozen samples, respectively. The differences between the medians and the average of the impact works are cc. 10% in the cases belongs to the samples of saturated normal and dry frozen rocks. The reason for this is that the water in the sample is also in a frozen state, thereby even strengthening the sample. On the other hand, if saturated samples are examined without freezing, the water saturation significantly worsens the impact resistance of the sample.

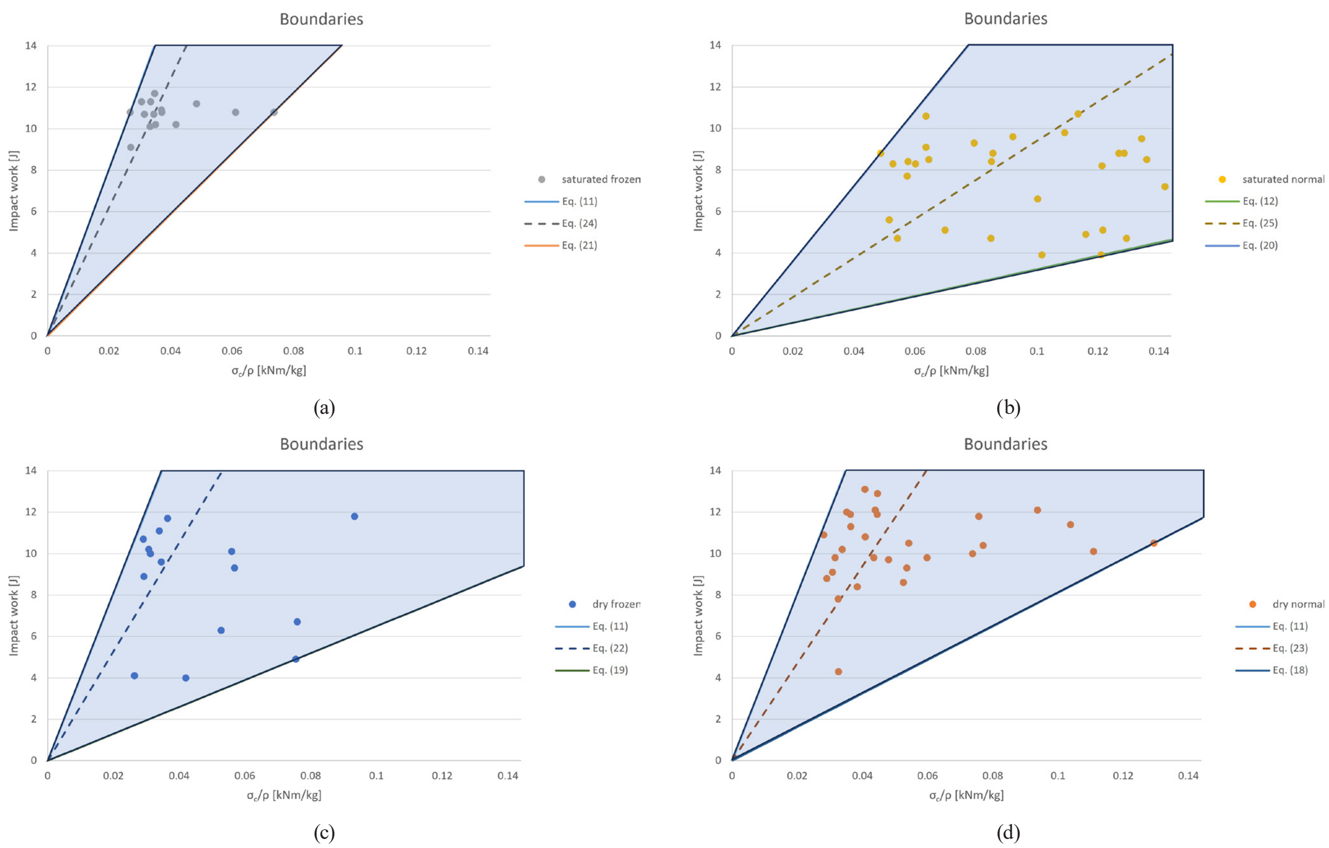

Fig. 11 Impact work in function of normalized compressive strength, where the boundaries (envelope lines) of each state: (a) saturated, frozen samples, (b) saturated, normal samples, (c) dry, frozen samples, (d) dry normal samples

Table 3 Impact work and uniaxial compressive strength in different conditions

	average		median		min		max	
	imp. res [J]	UCS [kN/m^2]	imp. res [J]	UCS [kN/m^2]	imp. res [J]	UCS [kN/m^2]	imp. res [J]	UCS [kN/m^2]
dry frozen	8.6	60.0	9.6	67.2	4	26.7	11.8	90.8
dry normal	10.2	53.7	10.3	54.7	4.3	18.7	13.1	86.8
saturated frozen	10.7	66.5	10.8	68.7	9.1	32.8	11.7	91.5
saturated normal	7.6	29.4	8.35	26.9	3.9	16.9	10.7	49.7

Based on the results above, it can be stated that in this temperature range, i.e. between −12 °C and 20 °C, the water saturation of the sample has a greater influence on the impact resistance than the temperature of the sample.

For each range, it becomes possible not only to define a lower and an upper limit curve (envelope lines) of the impact work for the given range, but also to give an expected estimate for the given state, using the median value of normalized compressive strength of the samples (Fig. 12). This estimate is given by Eq. (22) for the air-dry frozen state, Eq. (23) for the air-dry, normal state, Eq. (24) for the saturated frozen state, and Eq. (25) for the saturated normal state.

$$\sigma_c = 0.0037 \times \rho \times W \quad (22)$$

$$\sigma_c = 0.0043 \times \rho \times W \quad (23)$$

$$\sigma_c = 0.0032 \times \rho \times W \quad (24)$$

$$\sigma_c = 0.0106 \times \rho \times W \quad (25)$$

This relationship can also be determined for all samples, in this case regardless of temperature and saturation state (Eq. (26)):

$$\sigma_c = 0.0106 \times \rho \times W\ . \quad (26)$$

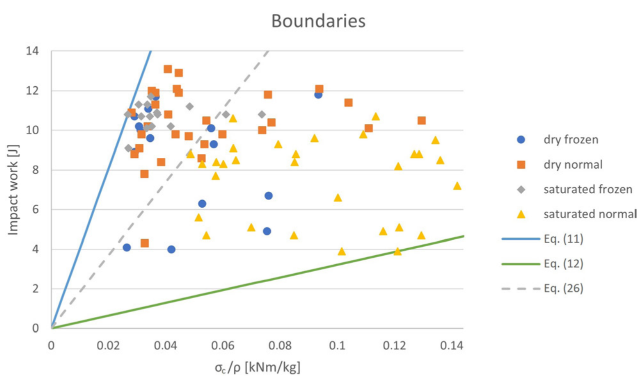

Fig. 12 Estimation of impact work based on the median value of the normalized compressive strength

One can see the evaluation of compressive strength in function of the impact work in Fig. 12.

During the optimal design procedures, one needs elliptic design domain of the data set to provide convexity of the feasible solutions. It also can demonstrate the uncertainty of the data set with this application. In this way the different sets of impact works–UCS data set were used to define this domain. A MATLAB code was written on the optimization principle, that the covered elliptic area should be minimal, while any of the measured points has to be inside the domain (under the ellipse). The following elliptic curves were determined: Fig. 13 all measured specimens, Fig. 14 saturated specimens and Fig. 15 dry specimens, respectively.

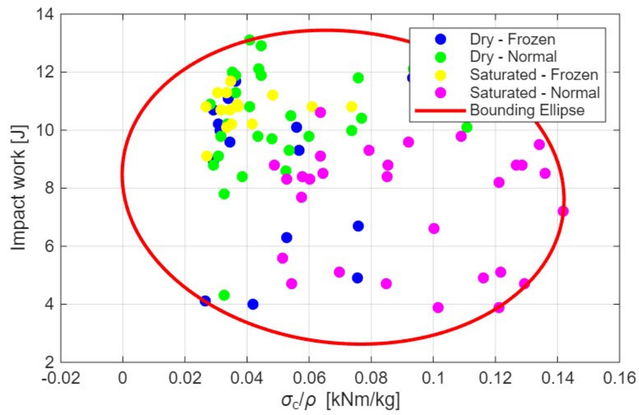

Fig. 13 Elliptic design domain for all points

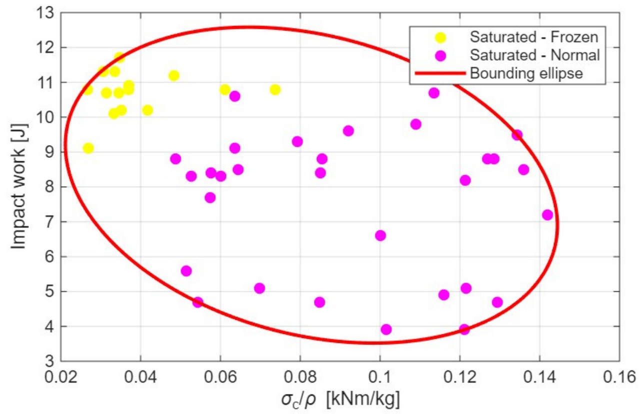

Fig. 14 Elliptic design domain for saturated specimens

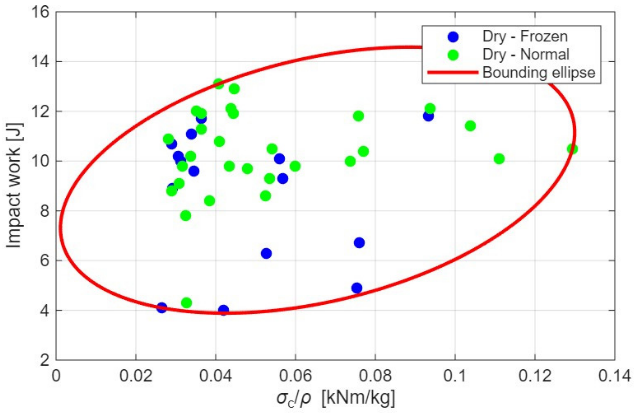

Fig. 15 Elliptic design domain for dry specimens

5 Conclusions

Based on the tests performed, it can be concluded that the Charpy impact test can also be used on sandstones, based on the measurement results, meaningful and clearly defined correlations can be seen. The lower and upper limits of the range of the measurement results can be determined regardless of the saturation state and temperature. By the use of these relationships, it is easy to determine either the compressive strength of the sedimentary rocks based on the knowledge of the impact work, or the impact work based on the knowledge of the compressive strength. The latter case can be useful for explosions, since the maximum and minimum required impact energy can be estimated with a simple relationship.

In addition to the boundary (envelope) lines the minimal elliptic design domains were also determined for the different saturation states. These domains are very useful in structural optimization, when the convexity of the design domain has to be provided.

Measurements performed at different temperatures and saturation states showed that the temperature of the sample at temperatures between −12 °C and 20 °C only minimally affects the result. The water saturation of the sample has a much greater effect on the impact resistance. Due to the ice in the samples, the impact resistance of the frozen, saturated sample either does not change compared to the impact energy of the air-dry sample or increases slightly.

Acknowledgement

The present paper was partially supported (B. A. Lógó) by the National Research, Development and Innovation Office (K138615).

References

[1] Charpy, G. "Essay on the Metals Impact Bend Test of Notched Bars (Reprint from 1901)", In: Siewert, T. A., Manahan, M. P., Sr. (eds.) Pendulum Impact Testing: A Century of Progress, ASTM International, 2000. ISBN 978-0-8031-2864-4
https://doi.org/10.1520/STP14386S

[2] Sankarapandian, S., Pramod, R., Kumar, S. M., Shanmugam, N. S. "Experimental and finite element analysis of Charpy impact, uniaxial tension and bending test of spin-arc welded carbon steel 1018 plate", Materialwissenschaft und Werkstofftechnik, 54(12), pp. 1673–1683, 2023.
https://doi.org/10.1002/mawe.202200224

[3] Tioua, T., Djeghader, D., Redjel, B. "The Mechanical properties and statistical analysis of the Charpy impact test using the Weibull distribution in jute-polyester and glass-polyester composites", Fracture and Structural Integrity, 16(62), pp. 326–335, 2022.
https://doi.org/10.3221/IGF-ESIS62.23

[4] Erkliğ, A., Oğuz, Z. A., Bozkurt, Ö. Y. "An experimental investigation on the Charpy impact response of glass/epoxy composites aged in seawater", The International Journal of Materials and Engineering Technology, 4(1), pp. 51–60, 2021.

[5] Komurlu, E. "An Experimental Study on Determination of Crack Propagation Energy of Rock Materials under Dynamic Impact and Static Loading Conditions", Hittite Journal of Science and Engineering, 6(1), pp. 1–6, 2019.
https://doi.org/10.17350/HJSE19030000126

[6] Cargill, J. S., Shakoor, A. "Evaluation of empirical methods for measuring the uniaxial compressive strength of rock", International Journal of Rock Mechanics and Mining Science & Geomechanics Abstracts, 27(6), pp. 495–503, 1990.
https://doi.org/10.1016/0148-9062(90)91001-N

[7] Zorlu, K., Gokceoglu, C., Ocakoglu, F., Nefeslioglu, H., Acikalin, S. "Prediction of uniaxial compressive strength of sandstones using petrography-based models", Engineering Geology, 96(3–4), pp. 141–158, 2008.
https://doi.org/10.1016/j.enggeo.2007.10.009

[8] Çobanoğlu, İ., Çelik, S. B. "Estimation of uniaxial compressive strength from point load strength, Schmidt hardness and P-wave velocity", Bulletin of Engineering Geology and the Environment, 67(4), pp. 491–498, 2008.
https://doi.org/10.1007/s10064-008-0158-x

[9] Fener, M., Kahraman, S., Bilgil, A., Gunaydin, O. "A Comparative Evaluation of Indirect Methods to Estimate the Compressive Strength of Rocks", Rock Mechanics and Rock Engineering, 38(4), pp. 329–343, 2005.
https://doi.org/10.1007/s00603-005-0061-8

[10] Borg, E. "New Impact test method for rock drill inserts", MSc Thesis, Uppsala University, 2018.

[11] Furuzumi, M., Sugimoto, F., Imai, T., Kamoshida, N., Abe, M. "岩石のシャルピー試験 (第1報) —動的破壊エネルギーについて—" (The Charpy Impact Test of Rock (1st Report) —Dynamic Fracture Energy—), Journal of Society of Materials Engineering for Resources of Japan, 18(1–2),pp. 10–14, 2006. (in Japanese) https://doi.org/10.5188/jsmerj.18.10

[12] Furuzumi, M., Sugimoto, F., Imai, T., Kamoshida, N., Abe, M. "岩石のシャルピー試験 (第2報) —動的破壊靭性について—" (The Charpy Impact Test of Rock (2nd Report) —Dynamic Fracture Toughness—), Journal of Society of Materials Engineering for Resources of Japan, 18(1–2), pp. 15–20, 2006. (in Japanese) https://doi.org/10.5188/jsmerj.18.15

[13] Durif, E., Réthoré, J., Combescure, A., Fregonese, M., Chaudet, P. "Controlling Stress Intensity Factors During a Fatigue Crack Propagation Using Digital Image Correlation and a Load Shedding Procedure", Experimental Mechanics, 52(8), pp. 1021–1031, 2012. https://doi.org/10.1007/s11340-011-9552-6

[14] He, C., Okubo, S., Nishimatsu, Y. "クラスII岩石の周圧下の挙動の載荷速度依存性" (Loading rate dependency of class II rock under confining pressure), Journal of the Society of Materials Science, Japan, 38(426), pp. 216–220, 1989. (in Japanese) https://doi.org/10.2472/jsms.38.216

[15] Kharchenko, V. V., Kondryakov, E. A., Zhmaka, V. N., Babutskii, A. A., Babutskii, A. I. "The effect of temperature and loading rate on the crack initiation and propagation energy in carbon steel Charpy specimens", Strength of Materials, 38(5), pp. 535–541, 2006. https://doi.org/10.1007/s11223-006-0073-y

[16] Zhang, Q. B., Zhao, J. "A Review of Dynamic Experimental Techniques and Mechanical Behaviour of Rock Materials", Rock Mechanics and Rock Engineering, 47(4), pp. 1411–1478, 2014. https://doi.org/10.1007/s00603-013-0463-y

[17] Zou, C., Wong, L. N. Y. "Experimental studies on cracking processes and failure in marble under dynamic loading", Engineering Geology, 173, pp. 19–31, 2014. https://doi.org/10.1016/j.enggeo.2014.02.003

[18] Protodyakonov, M. M. "Mechanical properties and drillability of rocks", In: Rock Mechanics: Proceedings of the Fifth Symposium on Rock Mechanics held at the University of Minnesota, May 1962, Mineapolis, MN, USA, 1963, pp. 103–118.

[19] Evans, I., Pomeroy, C. D. "The strength, fracture and workability of coal: A Monograph on Basic Work on Coal Winning Carried Out by the Mining Research Establishment, National Coal Board", Pergamon, 1966. ISBN 978-1-4831-9633-6 https://doi.org/10.1016/C2013-0-07718-3

[20] Charpy, M. G. "On testing metals by the bending of notched bars", International Journal of Fracture, 25(4), pp. 287–305, 1984. https://doi.org/10.1007/BF00963464

[21] Charpy, G. "Report on Impact Tests and the Work of Committee 26", In: Proceedings of the Sixth Congress of the International Association for Testing Materials, New York, NY, USA Vol. 4, 1912, pp. 1–10.

[22] Kahraman, S. "Evaluation of simple methods for assessing the uniaxial compressive strength of rock", International Journal of Rock Mechanics and Mining Sciences, 38(7), pp. 981–994, 2001. https://doi.org/10.1016/S1365-1609(01)00039-9

[23] Lógó, B. A., Vásárhelyi, B. "Charpy impact test procedure to sedimentary rocks", In: Fifth Symposium of the Macedonian Association for Geotechnics, Ohrid, Macedonia, 2022, pp. 839–844. ISBN 978-9989-2053-4-7

[24] Chatterjee, A., Chakrabarti, D., Moitra, A., Mitra, R., Bhaduri, A. K. "Effect of deformation temperature on the ductile–brittle transition behavior of a modified 9Cr–1Mo steel", Materials Science and Engineering: A, 630, pp. 58–70, 2015. https://doi.org/10.1016/j.msea.2015.01.076